Phycologia
2024, Volume 63, Issue 1, Pages 74-88
https://doi.org/10.1080/00318884.2023.2293311
https://archimer.ifremer.fr/doc/00868/98038/

A new dinoflagellate *Gonyaulax pospelovana* with resting cysts resembling *Spiniferites delicatus* and its biogeography and ecology revealed by DNA metabarcoding

Gu Haifeng [1, *], Zheng Jing [1], Huang Shuning [1], Morquecho Lourdes [2], Krock Bernd [3], Shin Hyeon Ho [4], Li Zhun [5], Derrien Amelie [6], Mertens Kenneth [6]

[1] Third Institute of Oceanography, Ministry of Natural Resources, Xiamen 361005, China
[2] Centro de Investigaciones Biológicas del Noroeste (CIBNOR), Av. IPN #195, Playa Palo de Sta. Rita Sur, La Paz, Baja California Sur 23096, Mexico
[3] Alfred Wegener Institute for Polar and Marine Research, Am Handelshafen 12, D-27570 Bremerhaven, Germany
[4] Library of Marine Samples, Korea Institute of Ocean Science and Technology, Geoje 53201, Korea
[5] Biological Resource Center/Korean Collection for Type Cultures (KCTC), Korea Research Institute of Bioscience and Biotechnology, Jeongeup 56212, Korea
[6] Ifremer, LITTORAL, F-29900 Concarneau, France

* Corresponding author : Haifeng Gu, email address : guhaifeng@tio.org.cn

Abstract :

Extant species of the dinoflagellate genus Gonyaulax are capable of producing resting cysts morphologically similar to different cyst-based genera, and their cyst-theca relationships are far from resolved. Here we have carried out germination experiments on several living cysts that resemble Spiniferites delicatus from the subtropical regions of China and Mexico. Both cyst and theca morphology were examined by light and scanning electron microscopy. A new species, Gonyaulax pospelovana, is described, characterized by a cingulum displacement and an overhang of twice its width, and two short antapical spines. The cysts of G. pospelovana had a granular surface and gonal processes with petaloid tips. Maximum likelihood and Bayesian inference analyses based on LSU and SSU rRNA gene sequences revealed that strains identified as G. pospelovana were monophyletic, forming a sister clade to Gonyaulax ellegaardiae and several presumable strains of Gonyaulax spinifera. One Chinese strain and two Mexican strains of G. pospelovana were examined for yessotoxin production using LC-MS/MS, but were not found to produce a detectable amount of toxins. Metabarcoding targeting the 18S V4 rRNA gene was performed on monthly collected samples in Xiamen Bay, China. A ZOTU (zero-radius operational taxonomic units) was detected that was consistent with G. pospelovana. Its maximum abundance was recorded in summer. Additionally, an OTU was identified as G. pospelovana from the Tara Oceans metabarcoding data, which occurred in the Indian and Pacific oceans at temperatures ranging from 28°C to 31°C, suggesting that it is a warm water species

Keywords : Cyst-theca relationship, Gonyaulax spinifera, 18S V4, Tara Oceans, Yessotoxin

INTRODUCTION

About 13%−16% of extant dinophyte species are known to have a cyst stage, which contribute to their dispersal, survival in adverse environmental conditions and even bloom initiation (Dale 1983; Head 1996). Cyst morphology is also helpful to differentiate species with conservative thecal morphology. A typical example is the groups of species attributed to the *Gonyaulax spinifera* species complex, which produce a variety of cysts resembling the fossil genera *Spiniferites* Mantell and *Nematosphaeropsis* Deflandre & Cookson (Rochon *et al*. 2009). *Spiniferites* cysts share the tabulation formula of 2pr, 4′, 6″, 6c, 5-6s, 6‴, 1p, 1⁗ but can be differentiated by size and shape of central body, number, location and shape of processes, the presence or absence of an apical boss, wall surface ornamentation, and cingular displacement (Mertens *et al*. 2018).

Among 107 currently accepted *Spiniferites* species (Williams *et al*. 2017; Gu *et al*. 2022), only 14 have been reported to be living (Zonneveld *et al.* 2013; Price & Pospelova 2014; Gu *et al*. 2022). The cyst-theca relationships of these 14 *Spiniferites* species have been investigated (Table S1), e.g. *S. bentorii* (M. Rossignol) D. Wall & B. Dale and *S. ramosus* (Ehrenberg) Mantell have been related to *Gonyaulax nezaniae* H. Gu & K.N. Mertens and *G. spinifera* (Claparède & J. Lachmann) Diesing, respectively (Lewis *et al*. 1999; Gu *et al*. 2021). However, new living *Spiniferites* cyst species can still be expected to be discovered as previous studies were limited to morphology obtained through light microscopy and current phylogenetics allows disentangling the species (Gu *et al*. 2022).

Some *Spiniferites* species bear gonal processes with a petaloid shape, such as *S. ristingensis* M.J. Head and *S. delicatus* P.C. Reid (Reid 1974; Head 2007). *Spiniferites*

delicatus was described from the British Isles (Reid 1974) and has been noted to dominate oligotrophic, hypersaline Aegean-Mediterranean water (Mudie *et al*. 2007). In contrast, it was also reported to be abundant in tropical waters and correlated with relatively low salinity (de Vernal *et al*. 2018), raising the concern that it could form a species complex. Recently, *S. pseudodelicatus* K.N. Mertens & H. Gu has been erected, based on phylogenetics and subtle differences from *S. delicatus*, such as the presence of intergonal processes in the former, and exclusively gonal processes in the latter (Gu *et al*. 2022). However, whether there are more hidden species resembling *S. delicatus* remains to be determined.

Irrespective of the cyst morphology (either resembling *Spiniferites* or *Impagidinium* Stover & Evitt) they produced, species of the *G. baltica* species complex form a monophyletic clade, characterized by numerous antapical short spines (Gu *et al*. 2022). The *G. spinifera* complex initially included *G. spinifera*, *G. digitale* (C.H.G. Pouchet) Kofoid and *G. diegensis* Kofoid (Kofoid 1911), but later more species were found with a similar morphology, including *G. nezaniae*, *G. membranacea* (M. Rossignol) Ellegaard, Daugbjerg, Rochon, Jane Lewis & I. Harding and *G. ellegaardiae* K.N. Mertens, H. Aydin, Y. Takano, A. Yamaguchi & Matsuoka. These species share two pronounced antapical spines of similar size (Ellegaard *et al*. 2003; Mertens *et al*. 2015; Gu *et al*. 2021). In contrast, *G. elongata* (P.C. Reid) Ellegaard, Daugbjerg, Rochon, Jane Lewis & I. Harding, *G. whaseongensis* A.S. Lim, H.J. Jeong & Ji Hye Kim and *G. taylorii* Carbonell-Moore show only one prominent antapical spine (Carbonell-Moore 1996; Ellegaard *et al.* 2003; Lim *et al*. 2018). Whether the number, shape and size of antapical spines are systematically meaningful in *Gonyaulax* species remains to be investigated.

Unfortunately, only a small fraction out of 85 currently accepted *Gonyaulax* species have molecular sequences available, since cultures are often difficult to establish for this group (Hernández-Becerril & Vega-Juárez 2022). In addition, molecular sequences are currently unavailable for some species able to produce yessotoxin (YTX), such as *G. taylorii* (Álvarez *et al.* 2016). On the other hand, strains identified as *G. spinifera* were genetically distinct and included both toxic and non-toxic strains (Riccardi *et al.* 2009; Chikwililwa *et al.* 2019), highlighting that more efforts are needed to clarify the taxonomy of *Gonyaulax* species.

Information on the ecology of *Gonyaulax* species is very scarce, except for several well-known bloom forming species (Amadi *et al*. 1992; Morton & Villareal 1998). This is not surprising considering the difficulty to differentiate *Gonyaulax* species from each other. However, the advent of molecular approaches holds promise, and DNA metabarcoding has been applied to reveal seasonal dynamics of protists in e.g. Skagerrak and Taiwan Strait (Gran-Stadniczeñko *et al.* 2019; Liu *et al*. 2023).

To pursue research into the cyst-theca relationships of *Gonyaulax* species, we isolated single cysts from China and Mexico and performed germination experiments to obtain LSU and/or SSU rRNA gene sequences of motile cells. Both cyst and theca morphologies were examined in detail with light microscopy (LM) and scanning electron microscopy (SEM), and the molecular phylogeny was inferred based on LSU and SSU rRNA gene sequences. In addition, a strain of *Gonyaulax* was examined for yessotoxin production by liquid chromatography coupled with tandem mass spectrometry (LC-MS/MS). We also tested the resolving power of the 18S V4 region for *Gonyaulax* species and utilized metabarcoding to

examine their seasonal occurrence in Xiamen Bay, and global biogeography was explored based on the Tara Oceans metabarcoding data of 18S V4 region (Vernette *et al*. 2021).

MATERIAL AND METHODS

Sample collection and treatment

Sediment sampling was taken with an Ekman grab in Xiamen Bay, China, in 2020 (Table 1). The top 2 cm of sediment were collected and stored in the dark at 4°C until further treatment. Approximately 5 g of wet sediment was mixed with 20 ml of filtered seawater and stirred vigorously to dislodge detrital particles. The settled material was subsequently sieved through 120 μm and 10 μm mesh, and washed and collected with filtered seawater. Single cysts were isolated using a micropipette with an inverted Eclipse TS100 (Nikon, Tokyo, Japan) microscope and incubated in 96-well plates with f/2-Si medium (Guillard & Ryther 1962) at 20°C and 90 μmol m^{-2} s^{-1}, under a 12:12 h light:dark cycle (hereafter called standard culture conditions). The Chinese strain is maintained in the culture collection of Third Institute of Oceanography, Ministry of Natural Resources and is available upon request. Water samples were also collected monthly at three stations in Xiamen Bay, from May 2018 to May 2019 (Table S2). One litre of water samples collected at 3 m and 10 m depth were mixed and prefiltered through a 200 μm mesh-size sieve, subsequently filtered onto 5 μm pore-size polycarbonate filters (Millipore, Eschborn, Germany) and stored at –20°C for DNA extraction.

Phytoplankton and sediment samples in Mexico were obtained from Bahía de La Paz in 2012 (BAPAZ), and from the southwestern end of Isla San José in 2014 (ISJ) (Table 1). In

BAPAZ phytoplankton was collected by vertical hauls with a 20 µm mesh net, immediately filtered (60 µm) to remove zooplankton, and transferred to a sterile culture container that was previously partially filled with f/2-Si culture medium. The living phytoplankton sample was kept in a thermal container and, once in the laboratory, in a culture room at *c.* 25°C until processing. In ISJ surface sediment was collected by scuba divers, the top 1–2 cm of sediment was placed in 50-ml plastic tubes that were filled with seawater and wrapped with aluminum foil to avoid exposure to air and light. Because annual seawater temperature at Isla San José ranges from 17°C to 30°C (Halfar *et al.* 2006), sediment samples were stored in the dark at 20°C ± 2°C to simulate natural conditions until processing. The strains were established by isolating vegetative cells or hatching living cysts, using the micropipette technique according to Andersen & Kawachi (2005) and Matsuoka & Fukuyo (2000), respectively. For the establishment and long-term maintenance of the Mexican strains, GSe culture medium was used (Doblin *et al.* 1999). The seawater salinity used to prepare culture media varied between 37 and 39. Established strains were grown at 25 ± 2°C, with 40 µmol m^{-2} s^{-1} photon irradiance (12:12 h light:dark cycle), which is one of the standard conditions defined for the Marine Dinoflagellate Collection (CODIMAR, for its acronym in Spanish). Mexican strains are deposited in CODIMAR (Morquecho & Reyes-Salinas 2004).

Morphological study of cysts and thecate stages

Cysts and motile cells of three strains were examined and photographed using a Zeiss Axio Imager light microscope (Zeiss, Göttingen, Germany) equipped with a Zeiss Axiocam HRc digital camera. Cells were stained with 1:100,000 SYBR Green (Sigma Aldrich) for the shape

and location of the nucleus and photographed using the above microscope with a Zeiss-38 filter set (excitation BP 470/40, beam splitter FT 495, emission BP 525/50). Cyst and vegetative cell size were measured on LM images.

For SEM, mid-exponential batch cultures of strains were concentrated with a Universal 320 R centrifuge (Hettich-Zentrifugen, Tuttlingen, Germany) at 850× *g* for 10 min at room temperature. Cells and cysts were fixed with Lugol's solution (2.5% final concentration). They were deposited on polycarbonate membrane filters (GTTP Isopore, 0.22 μm pore size; Millipore, Billerica, Massachusetts, USA), which were rinsed with distilled water. The filters were processed following the methods described in Chomérat & Couté (2008). They were dehydrated in a graded series of ethanol baths (15%–100%), critical-point-dried, attached to a stub using double-sided adhesive tape and coated with gold. The stubs were examined at the Station of Marine Biology in Concarneau, France, using a Sigma 300 Gemini (Zeiss, Oberkochen, Germany) field-emission SEM equipped with both a conventional Everhart-Thornley and an in-lens secondary electron detector at 1.5 kV (working distance of about 9.3 mm). Tabulation labelling follows the Kofoidean system (Kofoid 1909, 1911). Sulcal plate labelling follows Balech (1980) and Carbonell-Moore *et al.* (2022).

PCR amplifications and sequencing

Single cells were isolated into a 0.5-ml PCR tube and washed several times with sterile distilled water. They were frozen and thawed with liquid nitrogen twice and used for templates. Various regions of the ribosomal RNA (rRNA) genes including the SSU and partial LSU (D1–D6) were amplified using primer pairs specified previously and following

standard protocols (Gu *et al.* 2021). Newly obtained sequences were deposited in GenBank with accession numbers OR392571, OR400156, and OR394639 to OR394641.

Sequence alignment and phylogenetic analyses

Newly obtained LSU and SSU rRNA gene sequences were aligned with sequences of *Gonyaulax* species and related taxa available in GenBank. Sequences were aligned using the MAFFT v7.110 (Katoh & Standley 2013) online program (http://mafft.cbrc.jp/alignment/server/) with default settings. Alignments were manually checked with BioEdit v7.0.5 (Hall 1999). The final alignment consisted of 1,545 (LSU) and 1,872 (SSU) base pairs including introduced gaps. For Bayesian inference (BI), the program jModelTest (Posada 2008) was used to select the most appropriate model of molecular evolution with Akaike Information Criterion (AIC). Bayesian reconstruction of the data matrix was performed using MrBayes 3.2 (Ronquist & Huelsenbeck 2003) with the best-fitting substitution model GTR+G. Four Markov chain Monte Carlo (MCMC) chains ran for 2,000,000 generations, sampling every 1,000 generations. The first 10% of burn-in trees were discarded. A majority rule consensus tree was created in order to examine the posterior probabilities (BPP) of each clade. Maximum likelihood (ML) analyses were conducted with RaxML v7.2.6 (Stamatakis 2006) on the T-REX web server (Boc *et al.* 2012) using the best model, and bootstrap support (BS) was assessed with 1,000 replicates.

The above SSU rRNA gene sequences alignment were cut using the primers TAReuk454FWD1 and TarEukREV3 (Stoeck *et al*. 2010) to obtain the V4 region sequences.

Molecular phylogeny was inferred with maximum likelihood and bayesian inference to test the resolving power of V4 region sequences for *Gonyaulax* species.

Yessotoxin analysis

Cultures of strain TIO1278 were grown in 200-ml Erlenmeyer flasks under standard culture conditions. At stationary phase, determined via linear regression of log-transformed cell count time series, *c.* 10^5 cells were concentrated with a Universal 320 R centrifuge at 850× *g* for 10 min at room temperature. Algal pellets were transferred to 2-ml microcentrifuge tubes and stored at –20°C until analysis for quantification of intracellular YTX. Measurements were carried out by liquid chromatography (LC 1100, Agilent, Waldbronn Germany) coupled to tandem mass spectrometry (API 4000 QTrap, Sciex, Darmstadt Germany) as detailed in Wang *et al.* (2019). In brief, separation was performed on a reversed phase column with gradient elution from 40% aqueous methanol-acetonitrile mixture to 100% methanol-acetonitrile. Yessotoxins were screened in the negative mode by selected reaction monitoring (SRM) and 25 YTX variants were monitored by the transitions detailed in Sala-Pérez *et al*. (2016).

Cultures of strains GPJQ-1 and GPPV-1 were grown in 50-ml glass culture tubes following the previously described standard CODIMAR culture protocols. Once cultures reached early exponential phase (1.5–2 weeks), cells were concentrated by filtration (20 µm), and algal pellets, for quantification of intracellular YTX, were transferred to 1.5 ml microcentrifuge tubes and stored at –20°C until analysis. Measurements were carried out by liquid chromatography (UFLC XR, Shimadzu, Tokyo, Japan) coupled to tandem mass

spectrometry (API 4000 Qtrap, Sciex, Framingham, Massachusetts, USA) as detailed in Zhang *et al.* (2020). In brief, separation was performed on a reversed phase column under gradient elution. Water (A) and acetonitrile 90% (B), both containing 6.7 mM ammonium hydroxide, were used as mobile phases. Yessotoxins were screened in the negative mode by multiple reaction monitoring (MRM) and 27 YTX analogues were monitored by the transitions detailed in supplementary material of Zhang *et al*. (2020).

DNA extraction and Illumina sequencing

Genomic DNA of monthly collected water samples in Xiamen Bay was extracted using NucleoSpin®Soil Kit (Macherey-Nagel, Düren, Germany) following the manufacturer's protocol. The primers TAReuk454FWD1 and TarEukREV3 (Stoeck *et al*. 2010) were used for PCR amplification. For each sample, an identifying barcode was placed on the forward primer and a 34 cycle PCR using the TaKaRa Ex Taq (Takara, Dalian, China) was performed. The following PCR conditions were used: 95°C for 5 min, followed by 34 cycles of 95°C for 50 s, 47°C for 50 s and 72°C for 50 s, and a final elongation step at 72°C for 10 min. The library was built according to the standard protocol of NEBNext® Ultra™ DNA Library Prep Kit for Illumina® (New England Biolabs, Massachusetts, USA). The amplicons were sequenced using a HiSeq 2500 platform (Illumina) based on a paired-end strategy (2 × 250 bp).

The reads obtained from Hiseq sequencing were analysed using USEARCH v11.0.667 (Edgar 2013) and VSEARCH v2.14.2 (Rognes *et al*. 2016), and were filtered, dereplicated and denoised to remove low quality reads (error rate > 1%), short reads (< 140 bp), chimeras

and singleton reads (Edgar & Flyvbjerg 2015; Rognes *et al.* 2016). Reads were clustered to ZOTUs (zero-radius operational taxonomic units) according to 97% similarity and the most abundant read was selected as the representative read for each ZOTU (Edgar 2013). Finally, ZOTUs annotation was conducted on the representative read of each ZOTUs against the PR2 database with sequence of strain TIO1278 added (Guillou *et al*. 2012), with the similarity at a cut off level of 99% for annotation. ZOTUs with coverage values less than 90% were removed.

The biogeography and ecology of *Gonyaulax pospelovana* based on the Tara Oceans 18S V4 metabarcoding data

The complete 18S rRNA gene sequence of strain TIO1278 was submitted to https://oba.mio.osupytheas.fr. A homologous metabarcode sequence matching the strain TIO1278 exactly was obtained. The biogeography of the corresponding OTU was displayed in a world map, and covariation with environmental variables (temperatures, salinity, distance to coast, latitude) was analysed online (Vernette *et al*. 2021).

RESULTS

Morphology

The original cyst from the Xiamen Bay that yielded strain TIO1278 (Table 1) was ovoid, with a central body 37.4 µm long and 34.2 µm wide (Fig. 1). The archeopyle was not reduced, corresponding to plate 3″ (Fig. 2). Gonal processes were 3.8–7.4 µm in length (5.2 ± 1.4 µm, n = 5). They had petaloid tips with occasional perforations at the base, and connected by low ridges (Fig. 3). Sometimes one (rarely two) intergonal processes 4.4–5.9 µm long

with bifurcate tips were present (Fig. 3). The paracingulum descended with a displacement of its own width, without overhang. The parasulcus was weakly expressed. The cyst surface was coarsely granular (Fig. 4). The cyst from Mexico that yielded strain GPJQ-1 was spheroidal and with a diameter of 40 µm, larger than the Chinese specimens. Also its gonal processes were longer, being 11.2–12.8 µm long with petaloid tips (Fig. 5). Occasionally intergonal processes were observed (Fig. 6).

Motile cells of strain TIO1278 were 27.7–42.2 µm (32.9 ± 3.5 µm, n = 34) long and 21.8–36.4 µm (26.7 ± 3.2 µm, n = 34) wide. They had a pronounced apical horn and a more angled shoulder on the right (Fig. 7). The epitheca was conical and the hypotheca was trapezoidal. There were numerous banded chloroplasts in the periphery (Fig. 8). The cingulum width ranged from 2.0 to 3.3 µm. It was located in the equatorial part of the cell and descended about twice of its width and displayed an overhang of two widths (Fig. 10). Cells often had two antapical spines of similar size (Fig. 9). The antapical spines on the right were 1.2–3.0 µm long whereas the spines on the left were 1.0–3.0 µm long. A prominent ventral pore was present (Fig. 11), and a curved nucleus was located in the hypotheca (Fig. 12).

The theca had a sexiform gonyaulacoid tabulation (Fensome *et al*. 1993, text-fig. 64B) with an S-type ventral organization (Fensome *et al*. 1993, text-figs 82B, D) and neutral torsion (Fensome *et al*. 1993, text-fig. 83B) (Figs 13, 14). The plate formula was 2pr, *4′, 6″, 6C, 5S, *6‴, 2p, 1⁗. The cell surface was thick and faintly reticulated, with many trichocyst pores. The apical pore complex (apc) comprised a cover plate and a pore plate, surrounded by raised ridges of neighbouring plates (Fig. 16). Plates 1′ and *4′a and *4′p were narrow and

elongated, whereas plates 2′ and 3′ were large and occupied the dorsal part (Fig. 15). There was a ventral pore at the junction of plates 4′a and 4′p (Fig. 16). The angle between the major axis and a line joining the ends of the cingulum was approximately 30°. The precingular plates were similar in size except that plate 6″ was relatively smaller (Figs 15, 17). The postcingular plates were similar in size and plate 1‴′ was hexagonal and symmetrical, located in the middle of the hypotheca (Fig. 18). Plate 1p was narrow and elongated, and contacted the left side of the wider 2p (Fig. 19). The sulcus was narrow in the middle but wide at both ends (Fig. 20). It comprised of the anterior sulcal plate (Sa), the anterior left sulcal (Ssa) plate, the posterior left sulcal (Ssp), the right anterior sulcal plate (Sda) and right posterior sulcal plate (Sdp) (Figs 13, 19, 20).

The morphology of the cultured strains GPPV-1 and GPJQ-1 from Mexico was similar to that of Chinese strain TIO1278 (Figs 21–26). Cells of strain GPPV-1 were 33.3–41.0 µm (38.3 ± 2.3 µm, n = 14) long and 25.6–38.5 µm (31.3 ± 3.6 µm, n = 14) wide. Cells of strain GPJQ-1 were 28.2–38.5 µm (32.9 ± 2.6 µm, n = 25) long and 23.0–33.3 µm (26.6 ± 2.8 µm, n = 25) wide. The antapical spines on the right were 1.2–3.0 µm long whereas the left spines were 1.3–2.5 µm long. A schematic plate pattern is provided in Figs 27–30.

Molecular phylogeny

The two Mexican strains GPJQ-1 and GPPV-1 shared nearly identical LSU rRNA gene sequences (99.85% similarity), but differed from the Chinese strain TIO1278 at four positions (99.36% similarity). Strain TIO1278 differed from *Gonyaulax ellegaardiae*

(GenBank accession: LC036592) at 321 positions (70.36% similarity), and from an alleged *G. spinifera* strain (GenBank accession: DQ151557) at 281 positions (68.25% similarity).

ML and BI analyses based on LSU rRNA gene sequences yielded similar phylogenetic trees. The ML tree showed five well-resolved clades, corresponding to families Ceratiaceae, Protoceratiaceae, Pyrophacaceae, Gonyaulacaceae and Lingulodiniaceae (Fig. 31). Gonyaulacaceae was monophyletic with strong support (ML BS: 99, BPP: 0.94) and comprised two clades (clade I and clade II) . Clade II included *G. baltica* Ellegaard, Jane Lewis & I. Harding, *G. bohaiensis* H. Gu, K.N. Mertens & H.H. Shin, *G. amoyensis* H. Gu & K.N. Mertens and *G. portimonensis* K.N. Mertens, A. Amorim & H. Gu with strong ML support (98) but low BS posterior probability. Other *Gonyaulax* species were nested within clade I with maximal support. *Gonyaulax pospelovana* strains grouped together with maximal support (ML BS:100, BPP:1.0) and were sister to a clade comprising *G. ellegaardiae* and several presumable *G. spinifera* strains, with maximal support.

The ML tree based on SSU rRNA gene sequences was similar to that of LSU rRNA gene sequences (Fig. 32). Gonyaulacaceae likewise comprised two clades (clade I and clade II) with maximal support. *Gonyaulax pospelovana* resolved as sister to a clade comprising *G. digitale*, *G. ellegaardiae* and several alleged *G. spinifera* strains, with maximal support.

Yessotoxins

The strain TIO1278 of *G. pospelovana* was examined for production of YTXs. None of the 25 monitored YTX variants were detected in this strain. The detection limit was 0.046 pg

cell^{-1}. None of the 27 monitored YTX analogues were detected in the GPJQ-1 and GPPV-1 strains. The detection limit was 0.03 fg cell^{-1}.

Resolving power of 18S rDNA V4 domain for *Gonyaulax* species

A phylogenetic analysis comprising 438 bp and 69 sequences (including 19 *Gonyaulax* species) was performed. The ML tree showed that the majority of *Gonyaulax* appeared monophyletic (Fig. S1), with two exceptions: *Gonyaulax baltica* (GenBank accession: LC222300) was indistinguishable from *G. bohaiensis* (GenBank accession: OM177647), and *G. ellegaardiae* (GenBank accession: LC036590) was identical to a strain identified as *G. spinifera* (GenBank accession: EU805590). The 18S V4 domain was able to resolve most *Gonyaulax* at species level and thus were used in the subsequent metabarcoding approach.

Seasonal occurrence of *Gonyaulax pospelovana* in Xiamen Bay based on metabarcoding

ZOTUs of Gonyaulacaceae were detected from May 2018 to May 2019 targeting 18S rDNA V4 region. ZOTU6494 shared identical sequences with *Gonyaulax pospelovana*, and several ZOTUs of *G. baltica/bohaiensis*, *G. polygramma* and *G. ellargaardiae/spinifera* were also detected. The highest abundance of ZOTU6494 occurred in July 2018 and it was rare during other periods. ZOTU5086 was annotated as *G. polygramma* and mainly occurred in December 2018 (Fig. S2).

Biogeography and ecology of *Gonyaulax pospelovana* based on Tara Oceans metabarcode data

OTU17047 from the Tara Oceans 18S V4 metabarcode data was identical to a sequence of *Gonyaulax pospelovana*. OTU17047 was mainly detected in the Indian Ocean with the maximum relative abundance of $3.17 \times e^{-4}$ to $3.31 \times e^{-4}$. Its relative abundances were much lower in the Pacific Ocean, with the maximum relative abundance of $3.27 \times e^{-5}$ (Fig. 33). OTU17047 was mostly found in subsurface water samples and the maximum abundances were detected at temperatures of 28–31°C (Fig. S3). It was restricted to coastal waters (less than 300 m from the coast) and did not occur in latitudes above 25°.

DISCUSSION

Morphology

Cysts of *Gonyaulax pospelovana* from China and Mexico share gonal processes with petaloid tips and occasional intergonal processes with bifurcate tips. The processes of the Mexican specimen are longer than those of Xiamen Bay, possibly due to the relatively low salinity (*c*. 27) in Xiamen Bay and much higher salinity (*c*. 36) in Isla San José (Mertens *et al.* 2023). The negative relationship between process length and salinity has also been reported in cysts of *Gonyaulax baltica* and *Protoceratium reticulatum* (Claparède & J. Lachmann) Butschli (Ellegaard *et al*. 2002; Mertens *et al.* 2012). The cyst morphology of *G. pospelovana* is reminiscent of several species of *Spiniferites*, namely *S. delicatus*, *S. pseudodelicatus* and *S. ristingensis*. All of them share petaloid gonal processes and a microgranular wall, but cysts of *G. pospelovana* lack an apical boss in contrast to the presence of a low apical boss in the

other (Reid 1974; Head 2007; Gu *et al*. 2022). In addition, *S. delicatus* does not show intergonal processes and has a reduced archeopyle (Reid 1974). *Spiniferites pseudodelicatus* shares intergonal processes with cysts of *G. pospelovana* but has higher membraneous flanges and a reduced archeopyle (Gu *et al*. 2022). Moreover, cysts of *G. pospelovana* have a more coarse and reticulate surface compared with *S. pseudodelicatus. Spiniferites ristingensis* has small blisters on the surface and a displacement of three cingular widths, whereas cysts of *G. pospelovana* have a reticulate surface and a displacement of two cingular widths (Table 2).

Cells of *G. pospelovana* are similar to those of *Gonyaulax spinifera* complex in morphology. All of them share two antapical spines and a marked cingular overhang, but *G. pospelovana* can be separated from *G. spinifera* (cysts resembling *Spiniferites ramosus*) by the larger cingulum displacement and overhang (2.0 vs 1.0) (Lewis *et al*. 1999; Gu *et al*. 2021). Cells of *G. pospelovana* are nearly identical to those of *G.* cf. *spinifera* (cysts resembling *Spiniferites scabratus*) but differ in possessing a ventral pore (Gu *et al*. 2021). Cells of *G. pospelovana* are much smaller than those of *G. digitale* (27.7–42.2 vs 50–75 μm long), and have a larger cingular overhang (2.0 vs 1.0–1.3). Cells of *G. pospelovana* have a smaller cingular displacement than *G. nezaniae* (2.0 vs 3.0), and much shorter antapical spines (1–3 vs 2–11 μm long). Both *G. ellegaardiae* and *G. membranacea* have as many as four finned antapical spines and their cingular displacements are much larger (Table 3). In view of the morphological dissimilarity between the strains reported herein and previous species, we describe them as the new species *G. pospelovana* (see below).

Molecular phylogeny

Our results support that *Spiniferites*, as currently circumscribed, is polyphyletic as it is intermingled with *Impagidinium* (Gu *et al*. 2021, 2022). To date, only three *Spiniferites* (*Spiniferites delicatus*, *S. pseudodelicatus* and *S. ristingensis*) are known to have gonal processes with petaloid tips, whereas other *Spiniferites* bear gonal processes with slender trifurcate tips (Mertens *et al*. 2018). Cysts of *Gonyaulax pospelovana* likewise have gonal processes with petaloid tips, but the motile cells are distant from *G. amoyensis* and *G. portimonensis*, which have cysts with the morphology of *S. pseudodelicatus* and *S. ristingensis*, in both LSU and SSU rDNA-based trees (Figs 31, 32). It appears that process morphology has taxonomic value at the species level only. *Spiniferites delicatus* also has petaloid processes (Reid 1974), but has not yet been sequenced; it will be interesting to explore its phylogenetic relationship.

Our results showed two clades of *Gonyaulax* as previously reported (Gu *et al*. 2022). The number, shape and size of antapical spines of motile cells appear to be useful to characterize these clades. Clade I seems to be dominated by two pronounced antapical spines, whereas those of clade II are more inconspicuous. Antapical spines have been observed in thecate dinoflagellates frequently. However, the phylogenetic significance of antapical spines has not been fully investigated. Numerous stout antapical spines were reported in *Unruhdinium penardii* var. *robustum* (Qi Zhang, G.X. Liu & Z.Y. Hu) Gottschling and was considered a key feature to separate the variety from *Unruhdinium penardii* (Lemmermann) Gottschling (Zhang *et al*. 2011). The presence of antapical spines was regarded as unusual and differentiating *Scrippsiella spinifera* Honsell & M. Cabrini from other *Scrippsiella*

species (Honsell & Cabrini 1991). Presence of antapical spines also contributes to differentiate *Podolampas* F. Stein from other genera of the family Podolampadaceae (Carbonell-Moore 1994). It appears that antapical spines are variable in systematic significance depending on the taxonomic groups. Whether the two clades of *Gonyaulax* represent two distinct genera requires further study to decide.

Yessotoxin

Neither the Chinese strain (TIO1278) nor the Mexican strains (GPJQ-1, GPPV-1) of *Gonyaulax pospelovana* produced yessotoxins above of the detection limit of 46 fg cell^{-1} and 0.03 fg cell^{-1}, respectively. Previous reports on yessotoxin production of other *Gonyaulax* species indicate YTX cell quotas in the pg cell^{-1} range. For example, a strain of presumably *G. spinifera* from New Zealand produced YTXs of 94 pg cell^{-1} (Rhodes *et al.* 2006). Two strains of presumably *G. spinifera* from the Adriatic Sea produced YTXs of 5.4 and 37.0 pg cell^{-1} respectively (Riccardi *et al.* 2009), and three strains of presumably *G. spinifera* from the Benguela Current upwelling system produced YTXs of 15.0–134.3 pg cell^{-1} (Chikwililwa *et al*. 2019). On the other hand, *G. membranacea* from South Africa produced YTXs of 2.1 pg cell^{-1} (Pitcher *et al.* 2019). Given the fact that an YTX cell quota of *G. pospelovana* is two to three orders of magnitude lower than most YTX-producing species, we conclude that *G. pospelovana* is a non-toxic species, but more strains need to be tested in the future to confirm this conclusion.

Biogeography and Ecology

The information on the biogeography and ecology of *Gonyaulax* species is scarce except for a few relatively large and distinct species such as *Gonyaulax digitale* (McKenzie & Cox 1991) and *G. polygramma* (Morton & Villareal 1998). With the advent of high-throughput sequencing, it becomes popular to uncover the protist diversity and ecology using metabarcoding based on 18S rDNA sequences (de Vargas *et al*. 2015). The enrichment of 18S rDNA sequences database from six (Mordret *et al*. 2018) to 19 *Gonyaulax* species also offers a better chance to uncover *Gonyaulax* species. The findings of *G. pospelovana* in subtropical area of China and Mexico suggest that it is a warm water species. The metabarcoding results from Xiamen Bay, where it occurred mainly in summer when the water temperature was around 31°C, are consistent with the Tara oceans data where it was found at temperatures of 28–31°C. The biogeographical baseline data of *G. pospelovana* offers a good chance to track its potential northward dispersal under global warming. The peak of *G. polygramma* in Xiamen bay in December is contrary to previous reports on its blooms in Belize in May, 1995 and 1996 (Morton & Villareal 1998). However, *G. polygramma* comprises two ribotypes (Kim *et al*. 2022) and they may have ecological differentiation.

Formal taxonomic description

Gonyaulax pospelovana* H. Gu, Morquecho, Zhun Li, H.H. Shin & K.N. Mertens *sp. nov.

Figs 1–30

DESCRIPTION: Cells were 27–42 µm long and 22–36 µm wide with two short antapical spines. The epitheca was conical with pronounced shoulders. The cell surface was thick and faintly reticulated.

The cingulum descended about twice its width and had an overhang of two widths. Cells displayed a plate formula of 2pr, *4′, 6″, 6C, 5S, *6‴, 2p, 1⁗. There was a ventral pore at the junction of plates 4′a and 4′p. The angle between the major axis and a line joining the ends of the cingulum was approximately 30°. The cysts of *G. pospelovana* were ovoid to spheroidal, 37–40 µm in length. The paracingulum descended with a displacement of its width. The gonal processes were petaloid, 4–13 µm long, with perforations at the base. There was occasionally one (rarely two) intergonal process with bifurcate tips. The archeopyle was not reduced and corresponded to the third precingular plate. Cyst surface was coarsely granular.

HOLOTYPE: SEM stub of thecate cells from a culture established from a cyst extracted from sediment of Xiamen Bay, China, shown in Figs 13–20 and stored at the CEDiT (Centre of Excellence for Dinophyte Taxonomy) dinoflagellate type collection, Wilhelmshaven, Germany with the code CEDiT2023H166.

REFERENCE CYST: SEM stub of a single cyst extracted from surface sediment of Xiamen Bay, China, shown in Figs 1–4 and stored at the CEDiT dinoflagellate type collection, Wilhelmshaven, Germany with the code CEDiT2023H167.

TYPE LOCALITY: Xiamen Bay, China (East China Sea; 24°31.50′N, 118°4.55′E). Collection date: 22 November 2020 by Haifeng Gu.

HABITAT: Marine and planktonic.

ETYMOLOGY: The epithet '*pospelovana*' is in honour of Dr. Vera Pospelova for her significant contributions to dinoflagellate cyst taxonomy.

GENBANK ACCESSION: OR392571 and OR394639, respectively nuclear-encoded SSU and LSU rRNA gene sequence.

CONCLUSION

Germination of living cysts resembling *Spiniferites delicatus* from subtropical areas of China and Mexico yielded a new, non-toxic dinoflagellate species, *Gonyaulax pospelovana*,

suggesting that the diversity of both *Spiniferites* and *Gonyaulax* has been underestimated. The traditional approach of single cyst germination complemented by subsequent SEM observations are powerful to clarify the cyst-theca relationships of *Spiniferites*-like cysts. On the other hand, modern molecular approaches such as metabarcoding have proved useful for revealing the biogeography and ecology of novel dinoflagellate species once their reference data is available, such as reported here for *Gonyaulax pospelovana*.

ACKNOWLEDGEMENTS

The Regional Council of Brittany, the General Council of Finistère and the urban community of Concarneau-Cornouaille-Agglomération are acknowledged for the funding of the Sigma 300 FE-SEM of the Station of Marine Biology in Concarneau.

FUNDING

This work was supported by the the National Key Research and Development Program of China (2019YFE0124700), National Natural Science Foundation of China (42076085), and the management of Marine Fishery Bio-resources Center (2023) funded by the National Marine Biodiversity Institute of Korea. The Sigma 300 FE-SEM used in this study was funded by The Regional Council of Brittany, the General Council of Finistère and the Urban Community of Concarneau-Cornouaille-Agglomération. The isolation and maintenance in perpetuity of the strains from Mexico is supported by the Collection of Marine Dinoflagellates (CODIMAR) belonging to CIBNOR.

REFERENCES

Álvarez G., Uribe E., Regueiro J., Blanco J. & Fraga S. 2016. *Gonyaulax taylorii*, a new yessotoxins-producer dinoflagellate species from Chilean waters. *Harmful Algae* 58: 8–15.

Amadi I., Rao D.S. & Pan Y. 1992. A *Gonyaulax digitale* red water bloom in the Bedford Basin, Nova Scotia, Canada. *Botanica Marina* 35: 451–455.

Andersen R.A. & Kawachi M. 2005. Traditional microalgae isolation techniques. In: *Algal culturing techniques* (Ed. by R.A. Andersen), pp 83–100. Elsevier, Amsterdam, Netherlands.

Balech E. 1980. On the thecal morphology of dinoflagellates with special emphasis on circular and sulcal plates. *Anales del Centro de Ciencias del Mar y Limnologia, Universidad Nacional Autonomia de Mexico* 7: 57–68.

Boc A., Diallo A.B. & Makarenkov V. 2012. T-REX: a web server for inferring, validating and visualizing phylogenetic trees and networks. *Nucleic Acids Research* 40: W573–W579.

Carbonell-Moore M.C. 1994. On the taxonomy of the family Podolampadaceae Lindemann (Dinophyceae) with descriptions of three new genera. *Review of Palaeobotany and Palynology* 84: 73–99.

Carbonell-Moore M.C. 1996. On *Spiraulax jolliffei* (Murray et Whitting) Kofoid and *Gonyaulax fusiformis* Graham (Dinophyceae). *Botanica Marina* 39: 347–370.

Carbonell-Moore M.C., Matsuoka K. & Mertens K.N. 2022. Gonyaulacalean tabulation revisited using plate homology and plate overlap, with emphasis on the ventral area (Dinophyceae). *Phycologia* 61: 195–210.

Chikwililwa C., McCarron P., Waniek J.J. & Schulz-Bull D.E. 2019. Phylogenetic analysis and yessotoxin profiles of *Gonyaulax spinifera* cultures from the Benguela Current upwelling system. *Harmful Algae* 85: Article 101626.

Chomérat N. & Couté A. 2008. *Protoperidinium bolmonense* sp. nov. (Peridiniales, Dinophyceae), a small dinoflagellate from a brackish hypereutrophic lagoon (South of France). *Phycologia* 47: 392–403.

Dale B. 1983. Dinoflagellate resting cysts: "benthic plankton". In: *Survival strategies of the algae* (Ed. by G.A. Fryxell), pp 69–136. Cambridge University Press, Cambridge, UK.

de Vargas C., Audic S., Henry N., Decelle J., Mahé F., Logares R., Lara E., Berney C., Le Bescot N., Probert I. *et al*. 2015. Eukaryotic plankton diversity in the sunlit ocean. *Science* 348 (6237): 1–12.

de Vernal A., Eynaud F., Henry M., Limoges A., Londeix L., Matthiessen J., Marret F., Pospelova V., Radi T., Rochon A. *et al*. 2018. Distribution and (palaeo) ecological affinities of the main *Spiniferites* taxa in the mid-high latitudes of the Northern Hemisphere. *Palynology* 42: 182–202.

Doblin M., Blackburn S.I. & Hallegraeff G.M. 1999. Comparative study of selenium requirements of three phytoplankton species: *Gymnodinium catenatum*, *Alexandrium minutum* (Dinophyta) and *Chaetoceros* cf. *tenuissimus* (Bacillariophyta). *Journal of Plankton Research* 21: 1153–1169.

Edgar R.C. 2013. UPARSE: highly accurate OTU sequences from microbial amplicon reads. *Nature Methods* 10: 996–998.

Edgar R.C. & Flyvbjerg H. 2015. Error filtering, pair assembly and error correction for next–generation sequencing reads. *Bioinformatics* 31: 3476–3482.

Ellegaard M., Lewis J. & Harding I. 2002. Cyst–theca relationship, life cycle, and effects of temperature and salinity on the cyst morphology of *Gonyaulax baltica* sp. nov. (Dinophyceae) from the Baltic Sea Area. *Journal of phycology* 38: 775–789.

Ellegaard M., Daugbjerg N., Rochon A., Lewis J. & Harding I. 2003. Morphological and LSU rDNA sequence variation within the *Gonyaulax spinifera-Spiniferites* group (Dinophyceae) and proposal of *G. elongata* comb. nov. and *G. membranacea* comb. nov. *Phycologia* 42: 151–164.

Gran-Stadniczeňko S., Egge E., Hostyeva V., Logares R., Eikrem W. & Edvardsen B. 2019. Protist diversity and seasonal dynamics in Skagerrak plankton communities as revealed by metabarcoding and microscopy. *Journal of Eukaryotic Microbiology* 66: 494–513.

Gu H., Huo K., Krock B., Bilien G., Pospelova V., Li Z., Carbonell-Moore C., Morquecho L., Ninčević Ž. & Mertens K.N. 2021. Cyst-theca relationships of *Spiniferites bentorii*, *S. hyperacanthus*, *S. ramosus*, *S. scabratus* and molecular phylogenetics of *Spiniferites* and *Tectatodinium* (Gonyaulacales, Dinophyceae). *Phycologia* 60: 332–353.

Gu H., Mertens K.N., Derrien A., Bilien G., Li Z., Hess P., Séchet V., Krock B., Amorim A., Li Z. *et al*. 2022. Unraveling the *Gonyaulax baltica* species complex: cyst–theca relationship of *Impagidinium variaseptum*, *Spiniferites pseudodelicatus* sp. nov. and *S. ristingensis* (Gonyaulacaceae, Dinophyceae), with descriptions of *Gonyaulax bohaiensis* sp. nov, *G. amoyensis* sp. nov. and *G. portimonensis* sp. nov. *Journal of Phycology* 58: 465–486.

Guillard R.R.L. & Ryther J.H. 1962. Studies of marine planktonic diatoms. I. *Cyclotella nana* Hustedt and *Detonula confervacea* Cleve. *Canadian Journal of Microbiology* 8: 229–239.

Guillou L., Bachar D., Audic S., Bass D., Berney C., Bittner L., Boutte C., Burgaud G., de Vargas C., Decelle J. *et al*. 2012. The protist ribosomal reference database (PR^2): a catalog of unicellular eukaryote small sub-unit rRNA sequences with curated taxonomy. *Nucleic Acids Research* 41: D597–D604.

Gurdebeke P.R., Pospelova V., Mertens K.N., Dallimore A., Chana J. & Louwye S. 2018. Diversity and distribution of dinoflagellate cysts in surface sediments from fjords of western Vancouver Island (British Columbia, Canada). *Marine Micropaleontology* 143：12–29.

Halfar J., Godinez-Orta L., Mutti M., Valdez-Holguin J.E. & Borges J.M. 2006. Carbonates calibrated against oceanographic parameters along a latitudinal transect in the Gulf of California, Mexico. *Sedimentology* 53: 297–320.

Hall T.A. 1999. BioEdit: a user-friendly biological sequence alignment editor and analysis program for Windows 95/98/NT. *Nucleic Acids Symposium Series* 41: 95–98.

Head, M.J. 1996. Modern dinoflagellate cysts and their biological affinities. In: *Palynology: principles and applications* (Ed. by J. Jansonius & D.C. McGregor), pp 1197–1248. Dallas, Texas, USA.

Head M.J. 2007. Last interglacial (Eemian) hydrographic conditions in the southwestern Baltic Sea based on dinoflagellate cysts from Ristinge Klint, Denmark. *Geological Magazine* 144: 987–1013.

Hernández-Becerril D.U. & Vega-Juárez G. 2022. Morphology of the marine, planktonic, thecate dinoflagellate *Gonyaulax areolata* (Dinophyceae), a species causing red tides in the tropical Mexican Pacific. *Phycologia* 61: 595–605.

Honsell G. & Cabrini M. 1991. *Scrippsiella spinifera* sp. nov. (Pyrrhophyta): a new dinoflagellate from the northern Adriatic Sea. *Botanica Marina* 34: 167–175.

Katoh K. & Standley D.M. 2013. MAFFT multiple sequence alignment software version 7: improvements in performance and usability. *Molecular Biology and Evolution* 30: 772–780.

Kim H.J., Li Z., Gu H., Mertens K.N., Youn J.Y, Kwak K.Y., Oh S.-J., Shin K., Yoo Y.D., Lee W. & Shin H.H. 2022. *Gonyaulax geomunensis sp. nov.* and two allied species

(Gonyaulacales, Dinophyceae) from Korean coastal waters and East China Sea: morphology, phylogeny and growth response to changes in temperature and salinity. *Phycologia* 62: 48–67.

Kofoid C.A. 1909. On *Peridinium steini* Jörgensen, with a note on the nomenclature of the skeleton of the Peridinidae. *Archiv für Protistenkunde* 16: 25–47.

Kofoid C.A. 1911. Dinoflagellata of the San Diego region, IV. The genus *Gonyaulax* with notes on its skeletal morphology and a discussion of its generic and specific characters. *University of California Publication in Zoology* 8: 187–286.

Lewis J., Rochon A. & Harding I. 1999. Preliminary observations of cyst-theca relationships in *Spiniferites ramosus* and *Spiniferites membranaceus* (Dinophyceae). *Grana* 38: 113–124.

Lim A.S., Jeong H.J., Kwon J.E., Lee S.Y. & Kim J.H. 2018. *Gonyaulax whaseongensis* sp. nov. (Gonyaulacales, Dinophyceae), a new phototrophic species from Korean coastal waters. *Journal of phycology* 54: 923–928.

Liu M., Tillmann U., Ding G., Wang A. & Gu H. 2023. Metabarcoding revealed a high diversity of Amphidomataceae (Dinophyceae) and the seasonal distribution of their toxigenic species in the Taiwan Strait. *Harmful Algae* 124: Article 102404.

Matsuoka K. & Fukuyo Y. 2000. Guía técnica para el estudio de quistes de dinoflagelados actuales. WESTPAC-HAB/WESTPAC/ IOC, Tokyo, Japan. 30 pp.

McKenzie C.H. & Cox E.R. 1991. Spatial and seasonal changes in the species composition of armored dinoflagellates in the Southwestern Atlantic Ocean. *Polar Biology* 11: 139–144.

Mertens K.N., Bringué M., Van Nieuwenhove N., Takano Y., Pospelova V., Rochon A., de Vernal A., Radi T., Dale B., Patterson R.T. *et al*. 2012. Process length variation of the cyst of the dinoflagellate *Protoceratium reticulatum* in the North Pacific and Baltic-

Skagerrak region: calibration as an annual density proxy and first evidence of pseudo-cryptic speciation. *Journal of Quaternary Science* 27: 734–744.

Mertens K.N., Aydin H., Uzar S., Takano Y., Yamaguchi A. & Matsuoka K. 2015. Relationship between the dinoflagellate cyst *Spiniferites pachydermus* and *Gonyaulax ellegaardiae* sp. nov. from Izmir Bay, Turkey, and molecular characterization. *Journal of Phycology* 51: 560–573.

Mertens K.N., Van Nieuwenhove N., Gurdebeke P.R., Aydin H., Bogus K., Bringué M., Dale B., De Schepper S., de Vernal A., Ellegaard M. *et al.* 2018. The dinoflagellate cyst genera *Achomosphaera* Evitt 1963 and *Spiniferites* Mantell 1850 in Pliocene to modern sediments: a summary of round table discussions. *Palynology* 42: 10–44.

Mertens K.N., Morquecho L., Carbonell-Moore C., Meyvisch P., Gu H., Bilien G., Duval A., Derrien A., Pospelova V., Sliwińska K.K. *et al.* 2023. *Pentaplacodinium lapazense* sp. nov. from Central and Southern Gulf of California, a new non-toxic gonyaulacalean resembling *Protoceratium reticulatum*. *Marine Micropaleontology* 178: Article 102187.

Mordret S., Piredda R., Vaulot D., Montresor M., Kooistra W.H. & Sarno D. 2018. dinoref: a curated dinoflagellate (Dinophyceae) reference database for the 18S rRNA gene. *Molecular Ecology Resources* 18: 974–987.

Morquecho L. & Reyes-Salinas A. 2004. *Colección de dinoflagelados marinos (CODIMAR).* Centro de Investigaciones Biológicas del Noroeste, S.C. La Paz, Baja California Sur, México. https://www.cibnor.gob.mx/investigacion/colecciones-biologicas/codimar; searched on 27 April 2023.

Morton S.L. & Villareal T.A. 1998. Bloom of *Gonyaulax polygramma* Stein (Dinophyceae) in a coral reef mangrove lagoon, Douglas Cay, Belize. *Bulletin of Marine Science* 63: 639–642.

Mudie P.J., Marret F., Aksu A.E., Hiscott R.N. & Gillespie H. 2007. Palynological evidence for climatic change, anthropogenic activity and outflow of Black Sea water during the late

Pleistocene and Holocene: centennial-to decadal-scale records from the Black and Marmara Seas. *Quaternary International* 167: 73–90.

Pitcher G.C., Foord C.J., Macey B.M., Mansfield L., Mouton A., Smith M.E., Osmond S.J. & Van Der Molen L. 2019. Devastating farmed abalone mortalities attributed to yessotoxin-producing dinoflagellates. *Harmful Algae* 81: 30–41.

Posada D. 2008. jModelTest: phylogenetic model averaging. *Molecular Biology and Evolution* 25: 1253–1256.

Price A.M. & Pospelova V. 2014. *Spiniferites multisphaerus*, a new dinoflagellate cyst from the Late Quaternary of the Guaymas Basin, Gulf of California, Mexico. *Palynology* 38: 101–116.

Reid P. 1974. Gonyaulacacean dinoflagellate cysts from the British Isles. *Nova Hedwigia* 25: 579–637.

Rhodes L., McNabb P., De Salas M., Briggs L., Beuzenberg V. & Gladstone M. 2006. Yessotoxin production by *Gonyaulax spinifera*. *Harmful Algae* 5: 148–155.

Riccardi M., Guerrini F., Roncarati F., Milandri A., Cangini M., Pigozzi S., Riccardi E., Ceredi A., Ciminiello P. & Dell'Aversano C. 2009. *Gonyaulax spinifera* from the Adriatic sea: toxin production and phylogenetic analysis. *Harmful Algae* 8: 279–290.

Rochon A., Lewis J., Ellegaard M. & Harding I.C. 2009. The *Gonyaulax spinifera* (Dinophyceae) "complex": perpetuating the paradox? *Review of Palaeobotany and Palynology* 155: 52–60.

Rognes T., Flouri T., Nichols B., Quince C. & Mahé F. 2016. VSEARCH: a versatile open source tool for metagenomics. *PeerJ* 4: Article e2584.

Ronquist F. & Huelsenbeck J.P. 2003. MrBayes 3: Bayesian phylogenetic inference under mixed models. *Bioinformatics* 19: 1572–1574.

Sala-Pérez M., Alpermann T.J., Krock B. & Tillmann U. 2016. Growth and bioactive secondary metabolites of arctic *Protoceratium reticulatum* (Dinophyceae). *Harmful Algae* 55: 85–96.

Stamatakis A. 2006. RAxML-VI-HPC: maximum likelihood-based phylogenetic analyses with thousands of taxa and mixed models. *Bioinformatics* 22: 2688–2690.

Stoeck T., Bass D., Nebel M., Christen R., Jones M.D., Breiner H.W. & Richards T.A. 2010. Multiple marker parallel tag environmental DNA sequencing reveals a highly complex eukaryotic community in marine anoxic water. *Molecular Ecology* 19: 21–31.

Vernette C., Henry N., Lecubin J., de Vargas C., Hingamp P. & Lescot M. 2021. The Ocean barcode atlas: a web service to explore the biodiversity and biogeography of marine organisms. *Molecular Ecology Resources* 21: 1347–1358.

Wang N., Mertens K.N., Krock B., Luo Z., Derrien A., Pospelova V., Liang Y., Bilien G., Smith K.F., De Schepper S., Wietkamp S., Tillmann U. & Gu H. 2019. Cryptic speciation in *Protoceratium reticulatum* (Dinophyceae): evidence from morphological, molecular and ecophysiological data. *Harmful Algae* 88: Article 101610.

Williams G.L., Fensome R.A. & MacRae R.A. 2017. *DINOFLAJ3*. American Association of Stratigraphic Palynologists, Data Series no. 2. http://dinoflaj.smu.ca/dinoflaj3.

Zhang Q., Liu G. & Hu Z. 2011. Morphological differences and molecular phylogeny of freshwater blooming species, *Peridiniopsis* spp. (Dinophyceae) from China. *European Journal of Protistology* 47: 149–160.

Zhang W., Li Z., Mertens K.N., Derrien A., Pospelova V., Carbonell-Moore M.C., Bagheri S., Matsuoka K., Shin H.H. & Gu H. 2020. Reclassification of *Gonyaulax verior* (Gonyaulacales, Dinophyceae) as *Sourniaea diacantha gen*. et *comb. nov*. *Phycologia* 59: 246–260.

Zonneveld K.A., Marret F., Versteegh G.J., Bogus K., Bonnet S., Bouimetarhan I., Crouch E., Vernal A. de, Elshanawany R., Edwards L. *et al*. 2013. Atlas of modern dinoflagellate cyst distribution based on 2405 data points. *Review of Palaeobotany and Palynology* 191: 1–197.

LEGENDS FOR FIGURES

Figs 1–6. Light (LM) and scanning electron micrographs (SEM) of cysts of *Gonyaulax pospelovana sp. nov.* from China and Mexico.

Fig. 1. LM, high focus of ventral view of the Chinese empty cyst extract from surface sediment yielding strain TIO1278, showing the cingular displacement (arrows). Scale bar = 10 μm.

Fig. 2. LM, high focus of dorsal view of the same cyst in Fig. 1, showing the archeopyle (arrow). Scale bar = 10 μm.

Fig. 3. SEM, the same cyst in Fig. 1, showing the gonal petaloid processes and intergonal processes (arrows). Scale bar = 10 μm.

Fig. 4. SEM, the same cyst in Fig. 1, showing microgranuate surface. Scale bar = 4 μm.

Fig. 5. LM, mid focus of of the living cyst yielding strain GPJQ-1, showing the long petaloid processes. Scale bar = 20 μm.

Fig. 6. SEM, An empty cyst from Mexico, showing the archeopyle and an intergonal process (arrow). Scale bar = 10 μm.

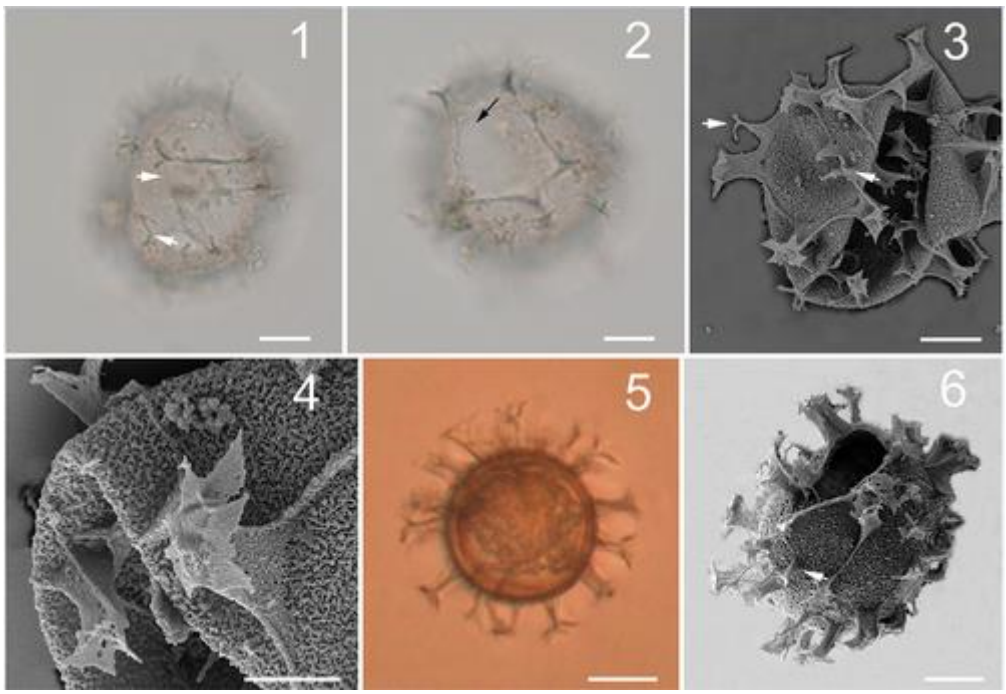

Figs 7–12. Motile cells from culture of *Gonyaulax pospelovana sp. nov.* strain TIO1278, LM. Scale bars = 10 μm.

Fig. 7. Mid focus of a living cell, showing the pronounced shoulder on the left side.

Fig. 8. High focus of a living cell, showing numerous bean-shaped chloroplasts.

Fig. 9. Mid focus of an empty theca, showing two stout antapical spines.

Fig. 10. Ventral view of an empty theca showing cingulum displacement.

Fig. 11. Apical-ventral view of an empty theca showing the ventral pore (arrow).

Fig. 12. A SYBR Green stained cell showing the nucleus (N).

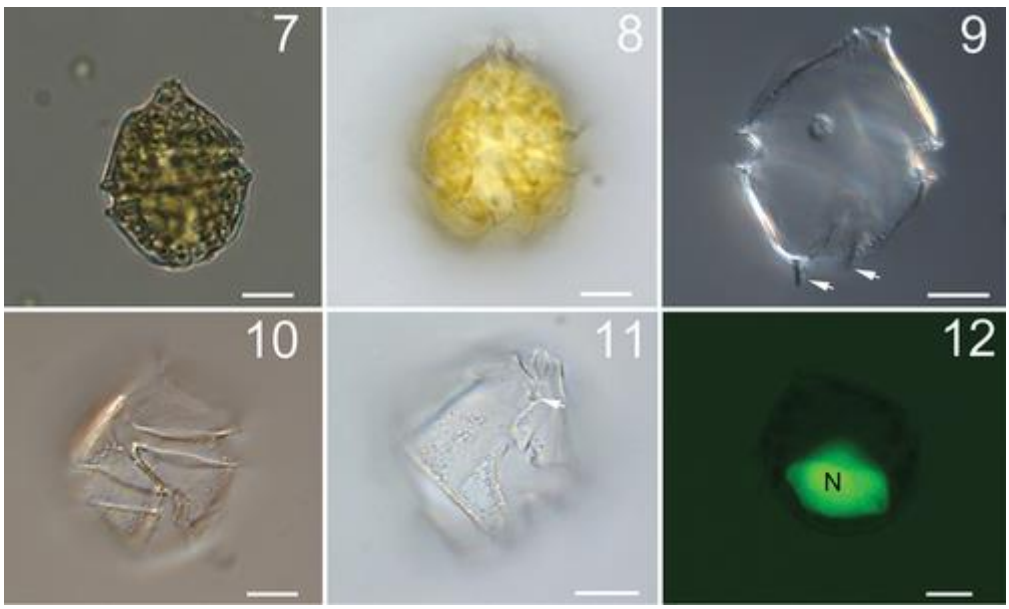

Figs 13–20. Motile cells from culture of *Gonyaulax pospelovana sp. nov.* strain TIO1278, SEM.

Fig. 13. Ventral view of a cell showing cingulum displacement, anterior sulcal plate (Sa) and the stout antapical spine (arrow). Scale bar = 10 μm.

Fig. 14. Dorsal view of a cell showing cingular plates (2c–5c), three precingular plates (2″–4″) and two postcingular plates (*4‴–*5‴). Scale bar = 10 μm.

Fig. 15. Apical view of a cell showing four apical plates (1′–4′) and six precingular plates (1″–6″). Scale bar = 10 μm.

Fig. 16. Ventral view of a cell showing a ventral pore (arrow) and the apical pore complex (apc). Scale bar = 2 μm.

Fig. 17. A broken cell showing four cingular plates (1c, 2c, 5c, 6c). Scale bar = 10 μm.

Fig. 18. Antapical view of a cell showing the five postcingular plates (*2‴–*6‴), one antapical plate (1⁗) and one posterior intercalary plate (1p). Scale bar = 10 μm.

Figs 19, 20. Ventral view showing the anterior sulcal plate (Sa), left anterior sulcal plate (Ssa), left posterior sulcal plate (Ssp), anterior right sulcal plate (Sda), posterior right sulcal plate (Sdp) and posterior sulcal plate (Sp). Scale bars = 5 μm.

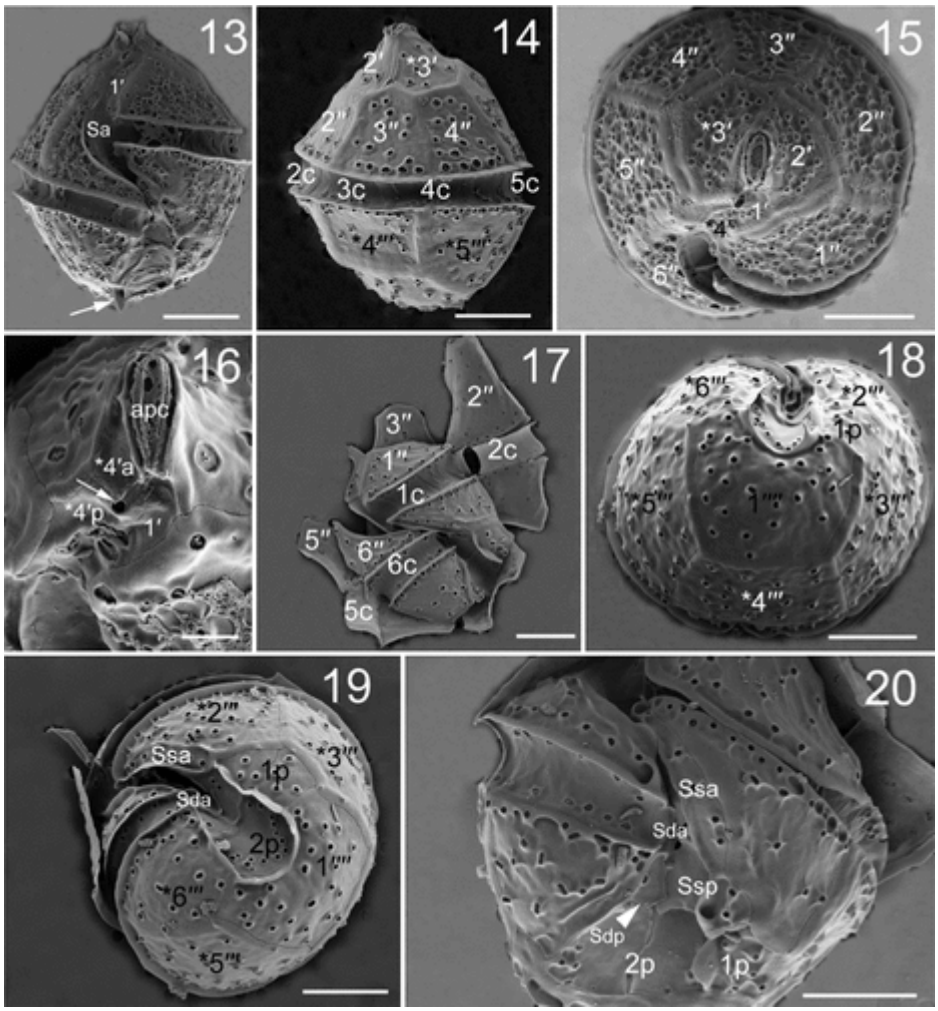

Figs 21–26. Motile cells from Mexican culture of *Gonyaulax pospelovana sp. nov.*, LM and SEM.

Fig. 21. Mid focus of a living cell, showing the pronounce shoulder in the left, LM. Scale bar = 10 μm.

Fig. 22. Ventral view of a cell showing cingulum displacement and the antapical spine (arrow, LM). Scale bar = 10 μm.

Fig. 23. Ventral view of a cell showing cingulum displacement and two short antapical spines (SEM). Scale bar = 10 μm.

Fig. 24. Apical view of a cell showing two apical plates (3′–4′) and six precingular plates (1″–6″) (SEM). Scale bar = 10 μm.

Fig. 25. Ventral view of a cell showing the first and fourth apical plates (1′, 4′), a ventral pore (arrow) and the apical pore complex (apc). Scale bar = 5 μm.

Fig. 26. Antapical view of a cell showing five postcingular plates (*2‴–*6‴), one antapical plate (1⁗) and one posterior intercalary plate (1p). Scale bar = 10 μm.

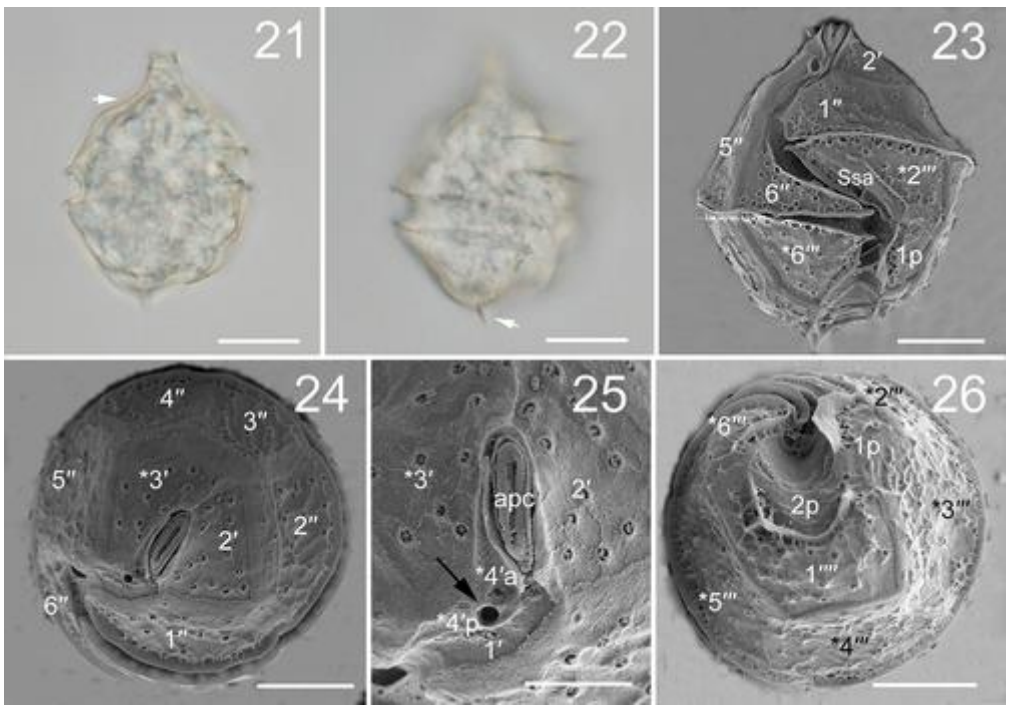

Figs 27–30. Schematic representation of motile cells of *Gonyaulax pospelovana sp. nov.*.

Fig. 27. Ventral view.

Fig. 28. Dorsal view.

Fig. 29. Apical view.

Fig. 30. Antapical view.

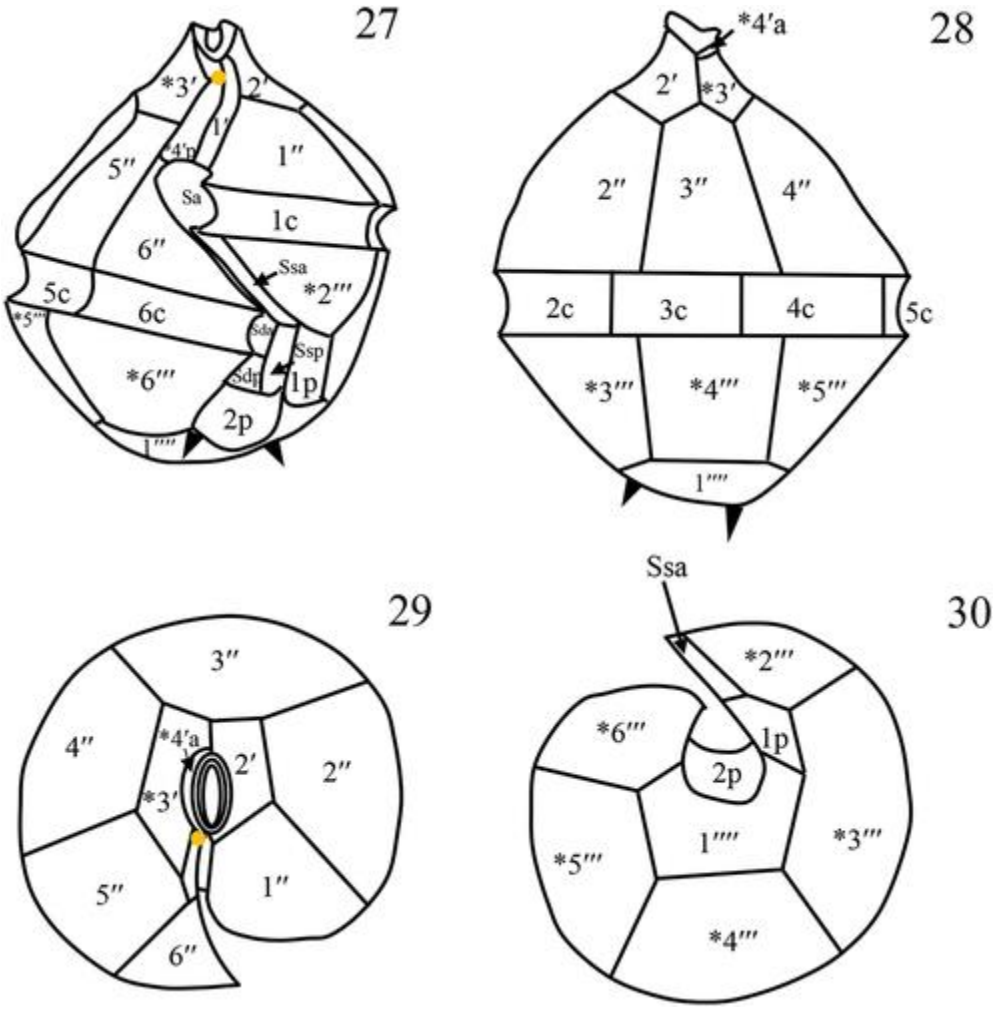

Fig. 31. Phylogeny of *Gonyaulax* inferred from partial LSU rRNA gene sequences using maximum likelihood (ML). New sequences indicated in bold. Five families labelled and marked with vertical lines on the right. Branch lengths drawn to scale, with scale bar indicating number of nucleotide substitutions per site. Numbers on branches are statistical support values to clusters on the right of them (left: ML bootstrap support values; right: Bayesian posterior probabilities). Only ML bootstrap support values above 50 and Bayesian posterior probabilities above 0.9 are shown. * indicates maximal support (ML bootstrap support: 100; BI posterior probability: 1.0).

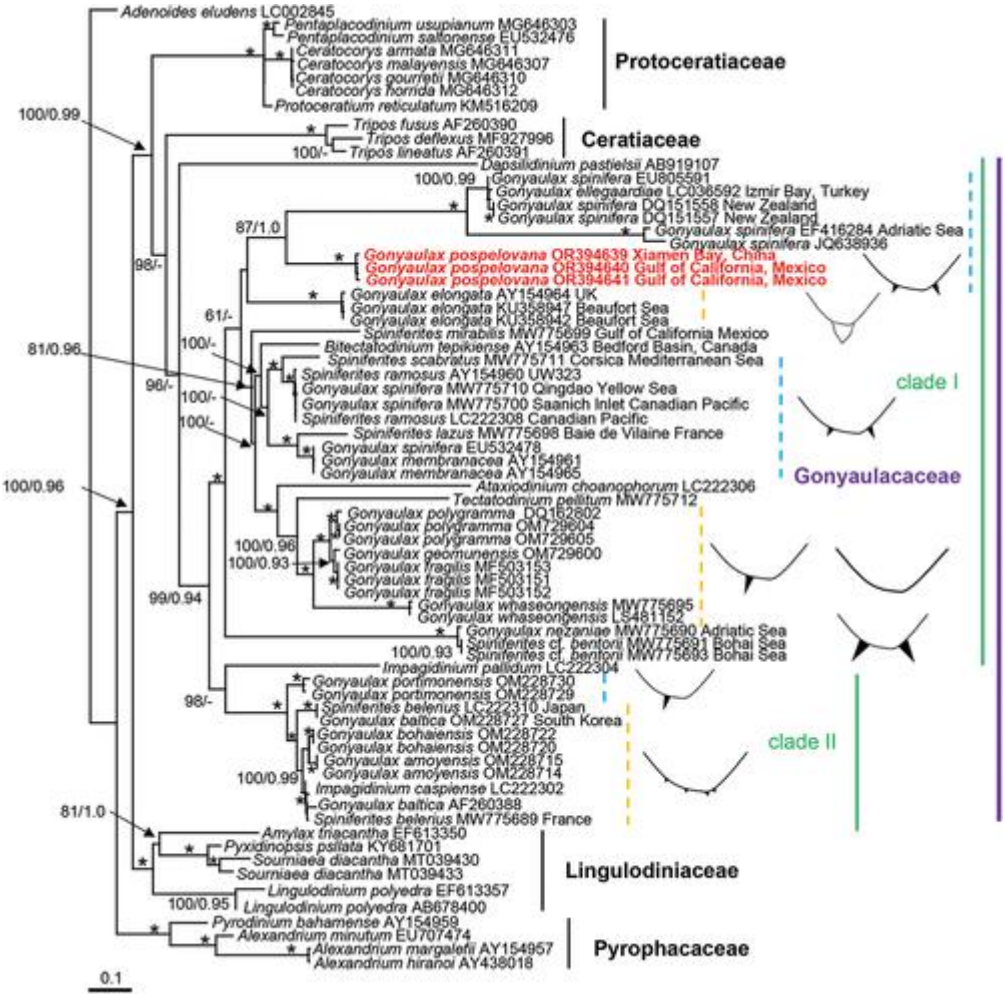

Fig. 32. Phylogeny of *Gonyaulax* inferred from partial SSU rRNA gene sequences using maximum likelihood (ML). New sequences indicated in bold. Five families labelled and marked with vertical lines on the right. Branch lengths drawn to scale, with scale bar indicating number of nucleotide substitutions per site. Numbers on branches are statistical support values to clusters on the right of them (left: ML bootstrap support values; right: Bayesian posterior probabilities). Only ML bootstrap support values above 50 and Bayesian posterior probabilities above 0.9 are shown. The dashed line indicates a half length. * indicates maximal support (ML bootstrap support: 100; BI posterior probability: 1.0).

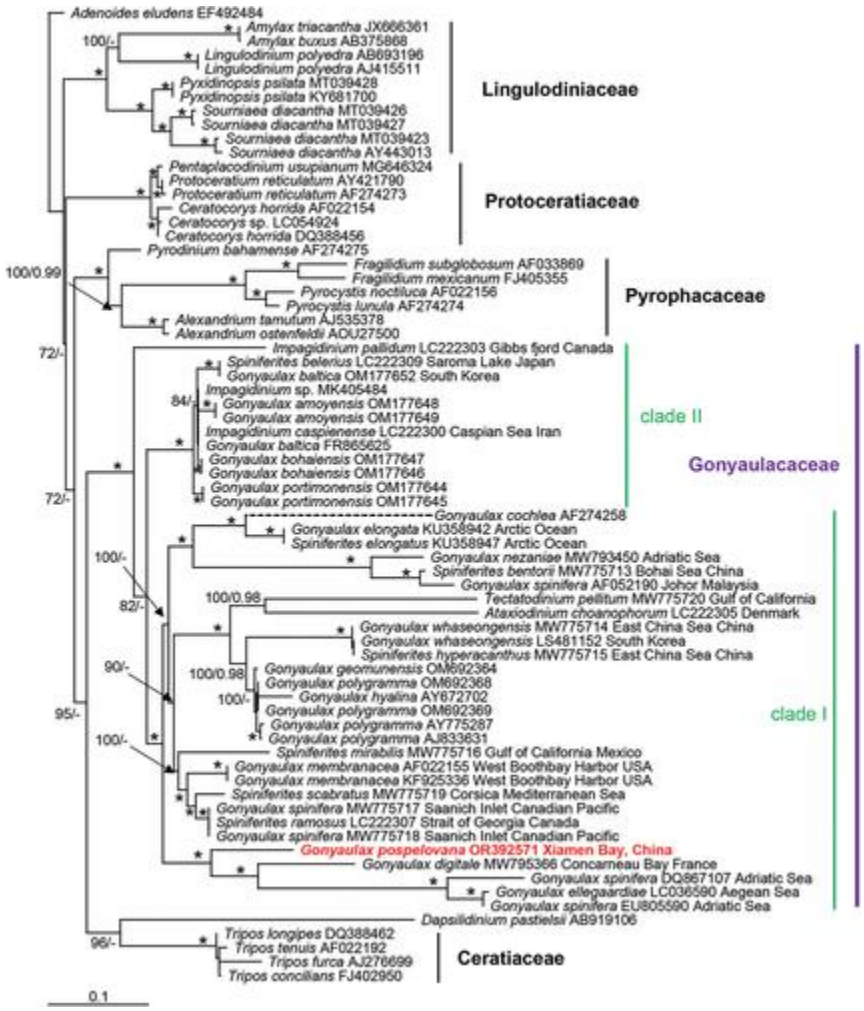

Fig. 33. Relative abundance of *Gonyaulax pospelovana sp. nov.* (OTU17047) from the Tara Oceans 18S V4 metabarcode data.